nature plants

Published: 29 July 2019

ARTICLES

https://doi.org/10.1038/s41477-019-0476-y

Non-invasive plant disease diagnostics enabled by smartphone-based fingerprinting of leaf volatiles

Zheng Li[1], Rajesh Paul[1], Taleb Ba Tis[2], Amanda C. Saville[3], Jeana C. Hansel[3], Tao Yu[1], Jean B. Ristaino[3,4] and Qingshan Wei[1,4]*

[1]Department of Chemical and Biomolecular Engineering, North Carolina State University, Raleigh, NC, USA. [2]Department of Materials Science and Engineering, North Carolina State University, Raleigh, NC, USA. [3]Department of Entomology and Plant Pathology, North Carolina State University, Raleigh, NC, USA. [4]Emerging Plant Disease and Global Food Security Cluster, North Carolina State University, Raleigh, NC, USA. *e-mail: qwei3@ncsu.edu

Affected by **late blight**

Paper Presentation
- Sritama Mukherjee
21.09.2019

GDCh Communications Angewandte International Edition Chemie

Analytical Methods

International Edition: DOI: 10.1002/anie.201705264
German Edition: DOI: 10.1002/ange.201705264

Colorimetric Recognition of Aldehydes and Ketones

*Zheng Li, Ming Fang, Maria K. LaGasse, Jon R. Askim, and Kenneth S. Suslick**

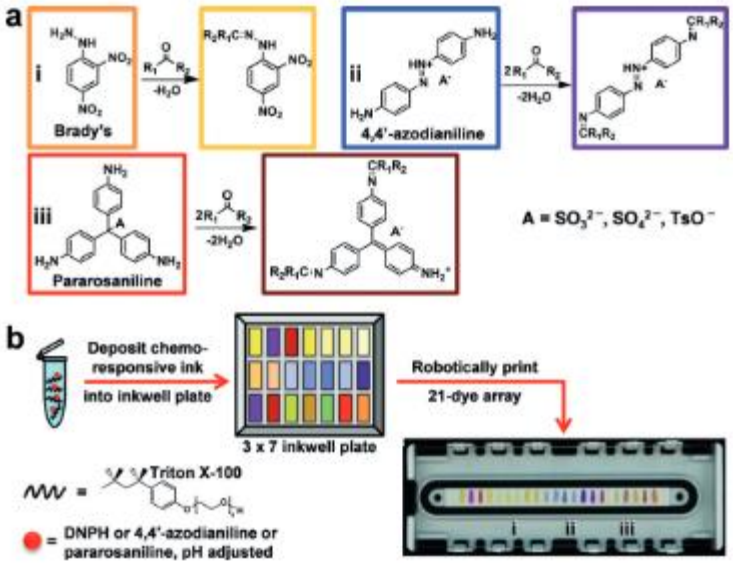

Figure 1. Designed aldehyde/ketone-responsive colorimetric sensor array. a) Three aldehyde/ketone-responsive dyes 2,4-dinitrobydrazine (i), 4,4′-azodianiline (ii) and pararosaniline (iii) with their color change reactions with carbonyl compounds. b) Preparation of a linearized 21-element sensor array.

ACS SENSORS

Article

pubs.acs.org/acssensors

Portable Optoelectronic Nose for Monitoring Meat Freshness

Zheng Li and Kenneth S. Suslick*

In this paper..

- VOC emission by plants has recently emerged as a non-invasive diagnostic marker of infectious plant diseases due to the rich chemical information of VOC and their unique functionality in plant self-defence and interplant communications.

- Non-invasive diagnosis of late blight caused by *Phytophthora infestans* by monitoring characteristic leaf volatile emissions in the field.

- A smartphone-integrated plant VOC profiling platform using a paper-based colourimetric sensor array that incorporates functionalized gold nanomaterials and chemo-responsive organic dyes for accurate and early detection of late blight in tomato leaves, for specific recognition of gaseous (E)-2-hexenal, one of the main VOC markers emitted during P. infestans infection.

- The multiplexed sensor array was scanned in real time by a three-dimensional (3D)-printed smartphone reader and calibrated with known concentrations of plant volatiles to provide quantitative information on volatile mixtures released by healthy and diseased plants.

- Using an unsupervised pattern-recognition method, this smartphone based VOC-sensing platform allows for the sub-ppm detection of (*E*)-2-hexenal and low-ppm discrimination of a range of disease related plant VOCs.

- Finally, the performance of the smartphone device was blind-tested using both laboratory-inoculated tomato leaves and field-collected infected leaves for detection of *P. infestans* and validated against PCR results.

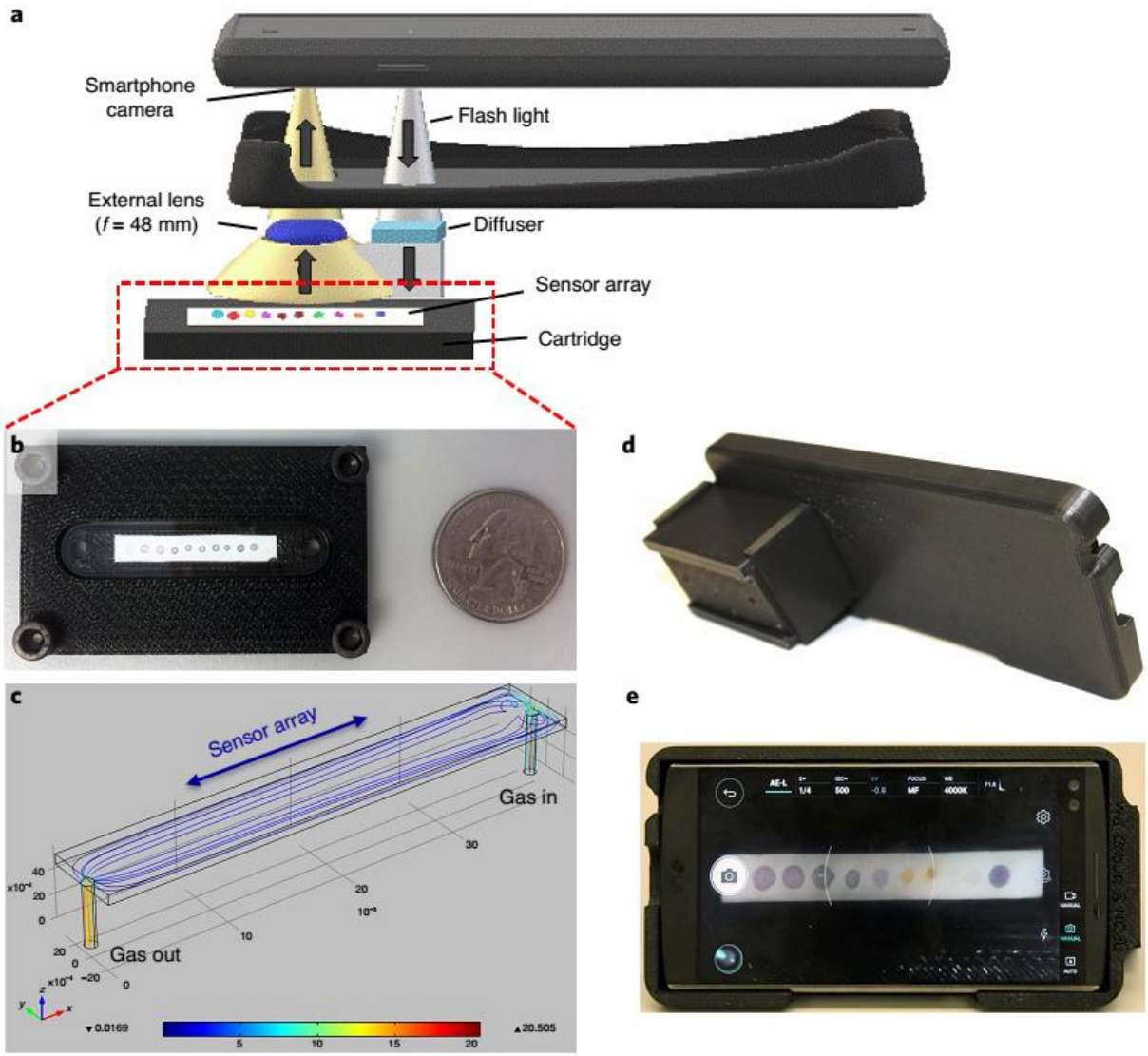

Fig. 1 | Design of the smartphone imaging platform for plant volatile sensing. **a**, Schematic representation of the smartphone device for sensor array scanning, consisting of a smartphone to provide light source and to capture images, a phone attachment with an external lens and a diffuser and a sensor cartridge containing the chemical sensor array. **b**, A photograph of the actual sensor cartridge with a loaded sensor array. **c**, COMSOL simulation of the gas flow in the array chamber. **d**,**e**, Photographs of the back (**d**) and front (**e**) of the smartphone-based VOC-sensing device.

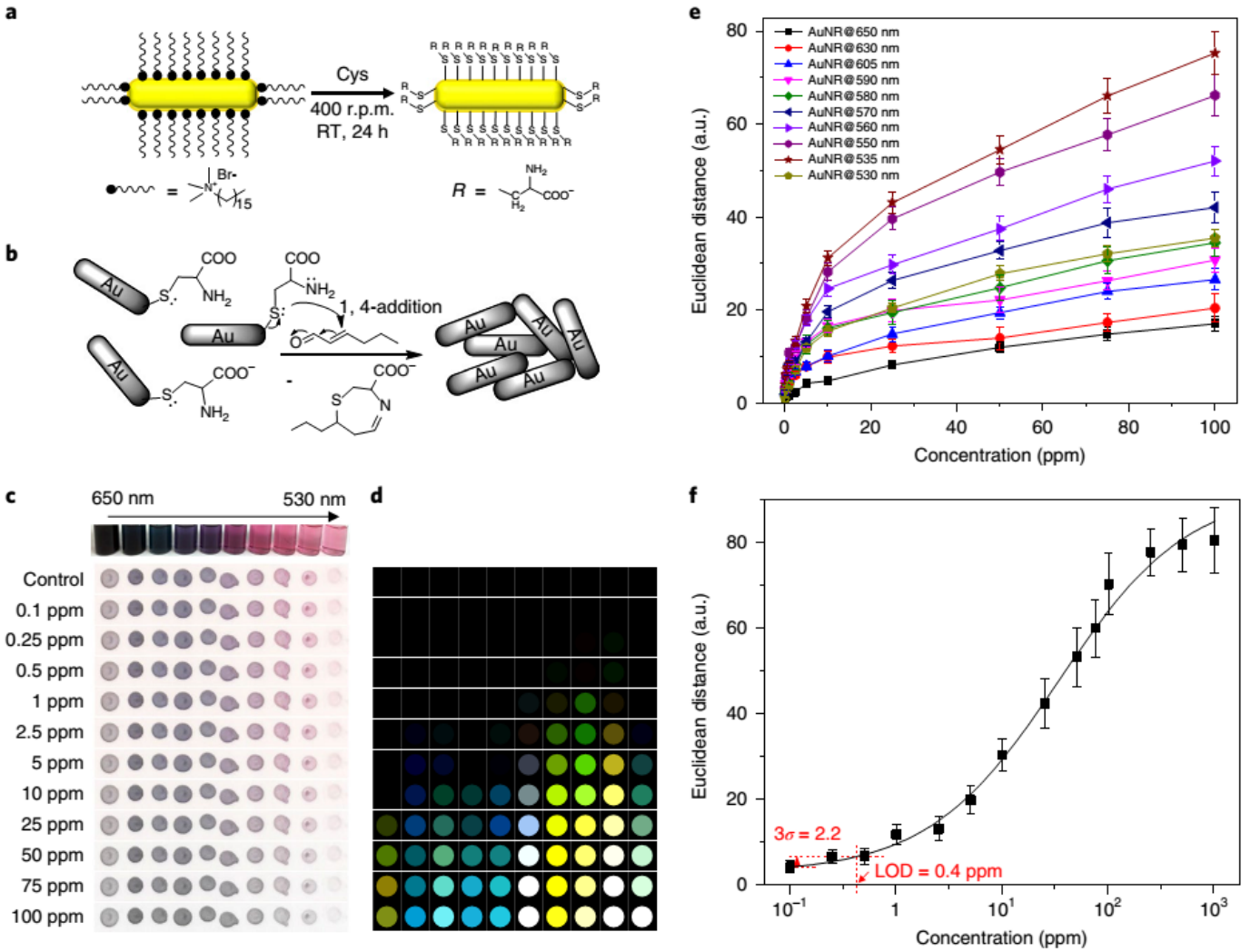

Fig. 2 | Vapour detection of the characteristic C6 plant aldehyde using functionalized Au NRs. **a**, Formation of Cys-capped Au NR via ligand exchange at room temperature (RT). **b**, Mechanism of the aggregation of Au NRs occurring at the gas–solid interface induced by exposure to (*E*)-2-hexenal. **c**, Before- and after-exposure smartphone images of various Cys–Au NR sensors following exposure of different vapour concentrations of (*E*)-2-hexenal (0.1–100 ppm) for 1 min; three measurements were repeated with similar results; inset shows a photograph of various Au NR inks in solution. **d**, Corresponding RGB differential images of each gas exposure; three replicates were averaged. For display purposes, the RGB colour range was rescaled from 3–10 to 0–255. **e**, Response curves of all Cys–Au NR sensors as a function of the vapour concentration of (*E*)-2-hexenal. **f**, LOD calculation of the most responsive sensor, Cys–Au NR with the absorption of 535 nm; the curve was fitted by an exponential function with $R_2 = 0.96$. A LOD of ~0.4 ppm was obtained on the basis of the Euclidean distance of a blank control (N_2 gas) plus three times the standard deviation (3σ) of the control (red dotted line). For **e** and **f**, data were presented as means ± s.d., $n = 3$ independent experiments. a.u., arbitrary unit.

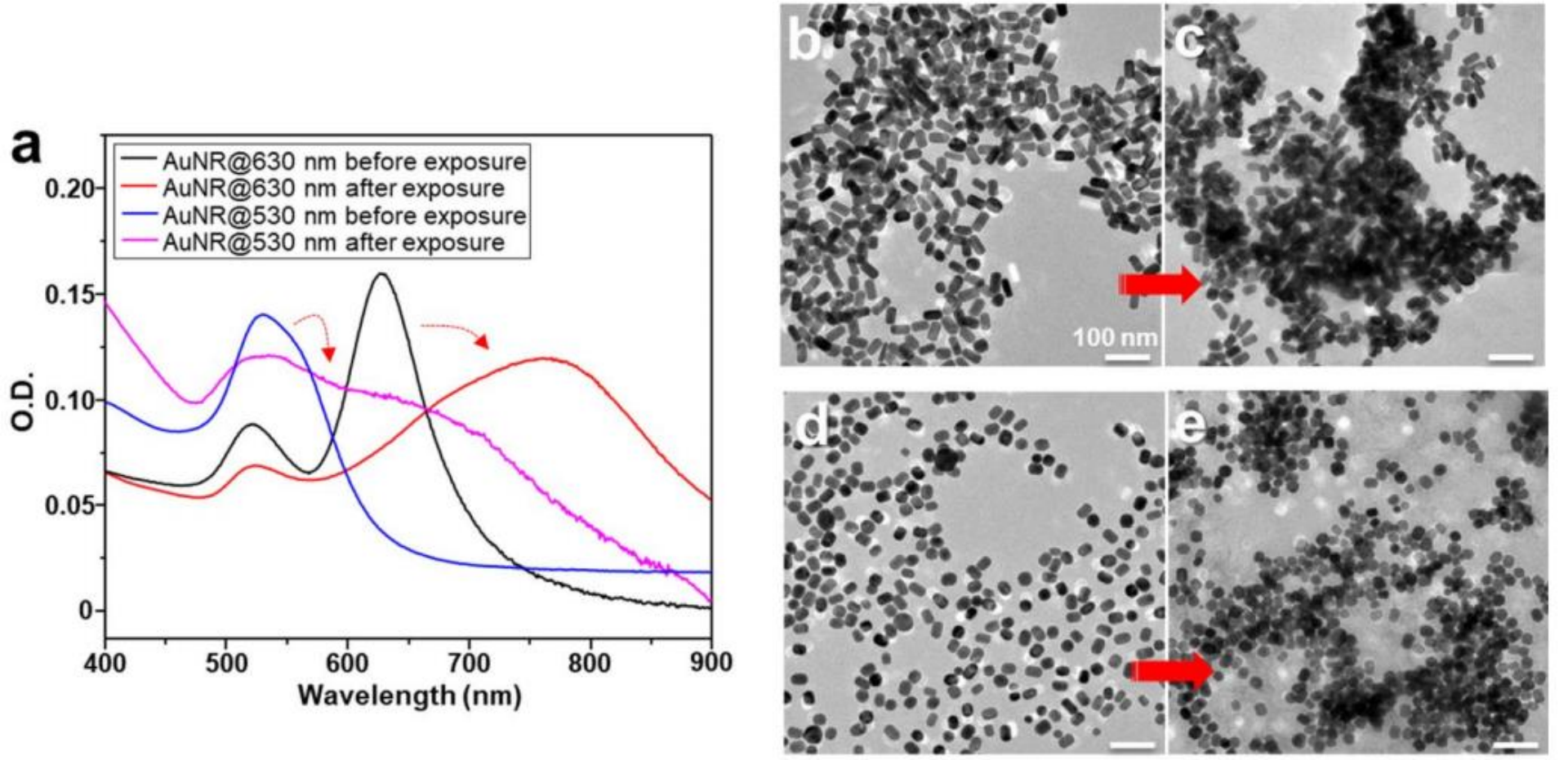

Figure S7. Optical properties and morphologies of Au nanomaterial sensors before and after vapor exposure. (a) UV-vis spectra of two Au NRs before and after exposure of 10 ppm gaseous (*E*)-2-hexenal for 1 min at the flow rate of 500 sccm; (b)-(e) TEM micrographs of Cys-Au NR@630 nm (b and c) and Cys-Au NR@530 nm (d and e) before and after the exposure to 10 ppm of (*E*)-2-hexenal. For TEM characterization, Cys-Au NRs were drop casted and dried on a TEM sample grid, which was then exposed to analyte prior to the acquisition of TEM images. For each sample, 3 measurements were repeated with similar results

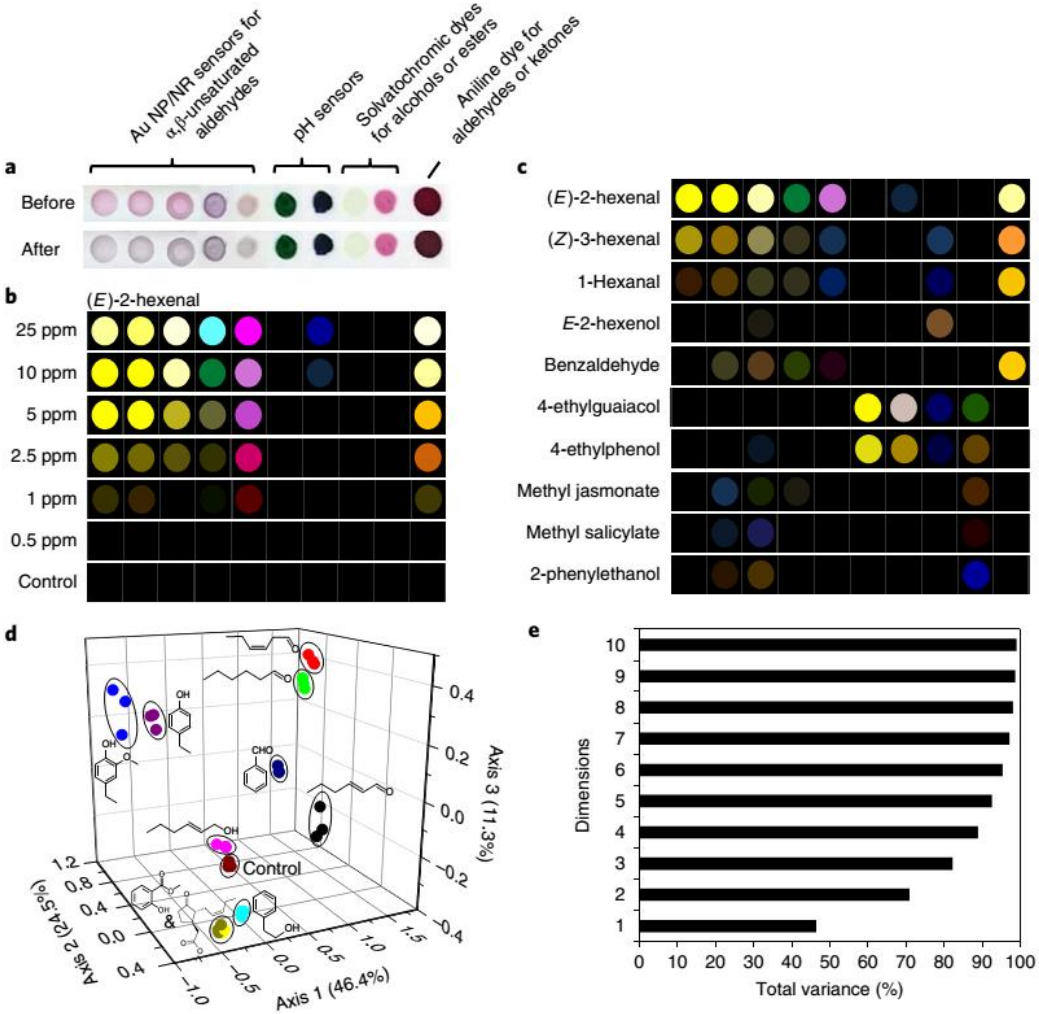

Table 1 | LODs of six representative plant volatiles detected by the chemical sensor array on the smartphone, as compared to the vapour levels detected in *P. infestans*-infected potato tissues by GC–MS

Plant VOCs	LODs (ppm)	Vapour level (ppm)[a]
(*E*)-2-Hexenal	0.4	12–18
(*Z*)-3-hexenal	1.1	6–12
1-hexanal	1.7	3–6
4-ethylphenol	1.8	3–6
Benzaldehyde	0.9	0.3–1.5
2-phenylethanol	5.2	1.5–3

[a]Data recalculated from ref. [25].

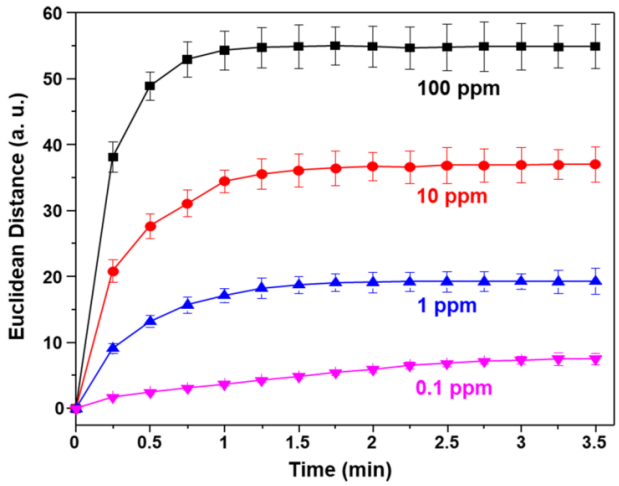

Fig. 3 | Sensor response of the multiplex array to ten major plant volatiles at the vapour level of 10 ppm for 1 min exposure and their chemometric analysis. **a**, Before- and after-exposure images of the ten-element sensor array in response to 10 ppm (*E*)-2-hexenal; three measurements were repeated with similar results. **b**, RGB differential profiles of the sensor array exposed to different concentrations of (*E*)-2-hexenal (0.5–25 ppm). **c**, RGB differential profiles of ten representative plant volatiles at 10 ppm. Each measurement is averaged over three replicates. For display purposes, the RGB colour range is rescaled from 3–10 to 0–255. **d**, PCA score plot using the first three principal components; all plant VOCs can be differentiated except for two weakly responding esters, jasmonate and salicylate; $n = 3$ independent experiments. **e**, PCA scree plot that recombines the RGB vectors of all ten sensor elements.
After recombination, only six dimensions are needed to account for >95% of total variance.

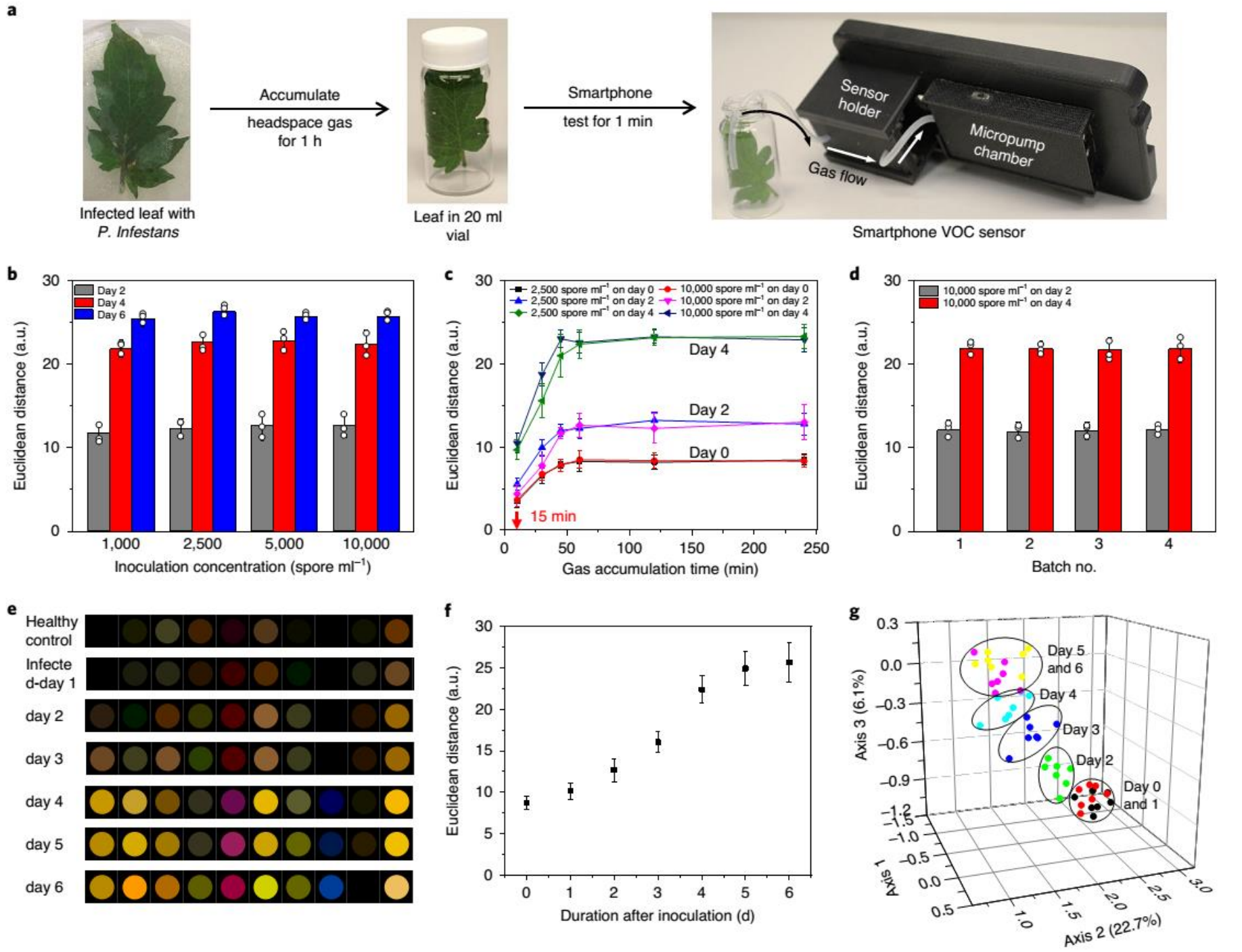
a
Infected leaf with P. Infestans
Accumulate
headspace gas
for 1 h
Leaf in 20 ml vial
Smartphone
test for 1 min
Sensor holder
Micropump chamber
Gas flow
Smartphone VOC sensor
b
Day 2
Day 4
Day 6
Euclidean distance (a.u.)
Inoculation concentration (spore ml−1)
1,000
2,500
5,000
10,000
c
2,500 spore ml−1 on day 0
2,500 spore ml−1 on day 2
2,500 spore ml−1 on day 4
10,000 spore ml−1 on day 0
10,000 spore ml−1 on day 2
10,000 spore ml−1 on day 4
Day 4
Day 2
Day 0
15 min
Euclidean distance (a.u.)
Gas accumulation time (min)
d
10,000 spore ml−1 on day 2
10,000 spore ml−1 on day 4
Euclidean distance (a.u.)
Batch no.
e
Healthy control
Infected-day 1
day 2
day 3
day 4
day 5
day 6
f
Euclidean distance (a.u.)
Duration after inoculation (d)
g
Day 5 and 6
Day 4
Day 3
Day 2
Day 0 and 1
Axis 3 (6.1%)
Axis 1
Axis 2 (22.7%)

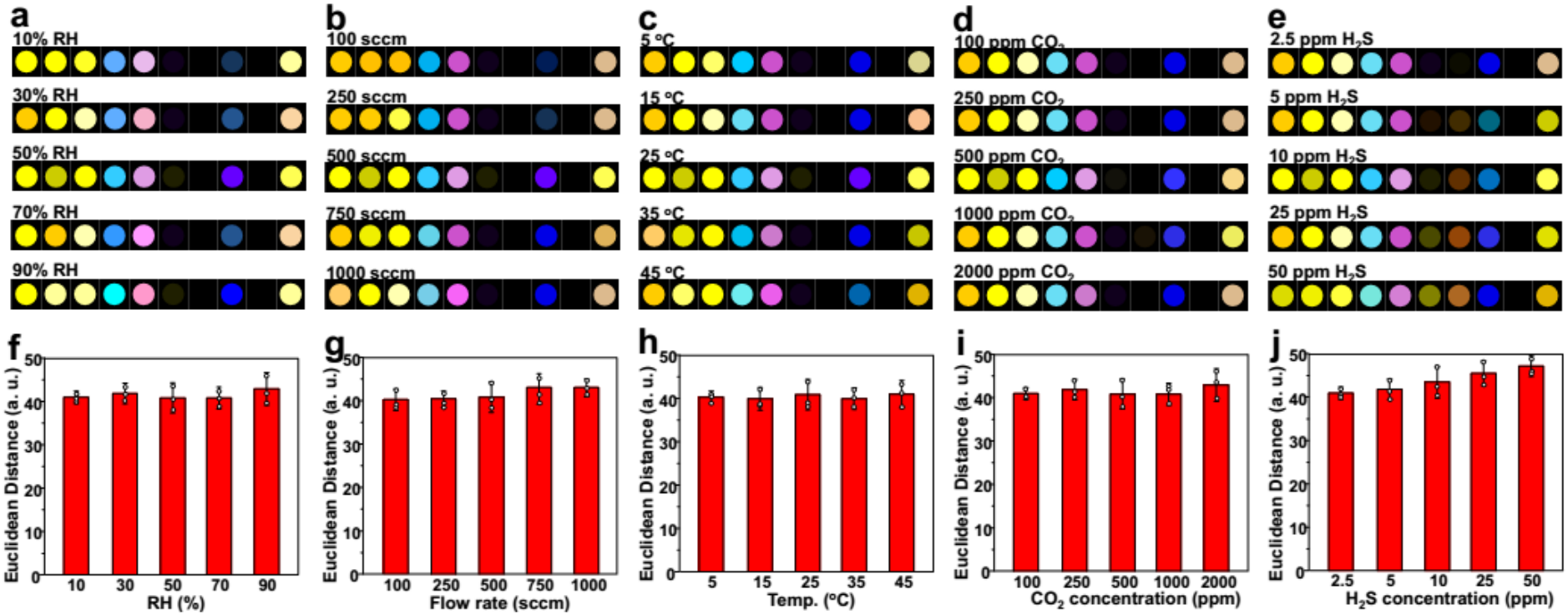

Figure S15. Evaluation of the sensor response stability of the colorimetric sensor array against various environmental factors. (a–e) Sensor array response to 10 ppm (*E*)-2-hexenal at different humidity (10–90% relative humidity), gas flow rates (100–1000 sccm), temperatures (5–45 $_{o}$C), and in the presence of interfering gas analytes, CO_2 and H_2S. (f–j) Bar graphs showing the corresponding sensor responses of each factor, as represented in Euclidean distances. Data were presented as means ± s.d., n=3 independent experiments.

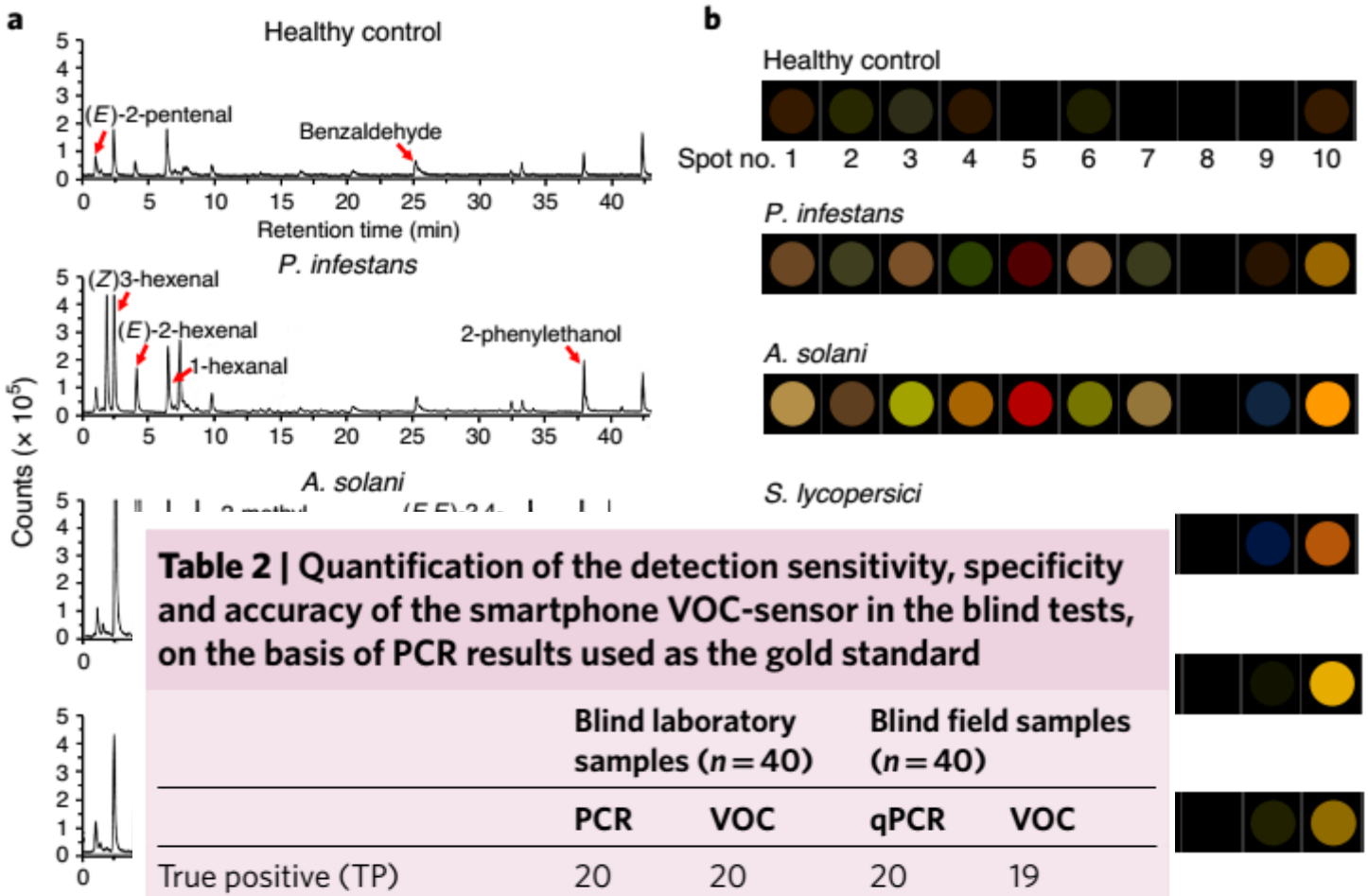

Table 2 | Quantification of the detection sensitivity, specificity and accuracy of the smartphone VOC-sensor in the blind tests, on the basis of PCR results used as the gold standard

	Blind laboratory samples ($n = 40$)		Blind field samples ($n = 40$)	
	PCR	**VOC**	**qPCR**	**VOC**
True positive (TP)	20	20	20	19
False positive (FP)	-	2	-	0
True negative (TN)	20	18	20	20
False negative (FN)	-	0	-	1
Sensitivity (TP/P)	-	100%	-	95%
Specificity (TN/N)	-	90%	-	100%
Accuracy ((TP + TN)/n))	-	95%	-	97.5%

Fig. 5 | Validation of the s from headspace of three infected tomato leaves a **b**, Differential RGB profiles of uninfected tomato leaves y leaves.

Conclusion

- Used plasmonic nanostructures analysed on a conventional chemical sensor array integrated a portable smartphone reader to facilitate field deployment and implementation

- The detection specificity of plasmonic gas sensors is achieved by the capturing ligands immobilized on the surface of nanostructures, therefore allowing versatile ligand design to extend the applications to a broad range of gaseous targets.

- The gas sample processing steps in our approach are relatively simple. The use of glass vials for collecting leafy headspace gas from detached samples provides a stable and reproducible testing environment.

- The device has been beta-tested in the greenhouse setting for monitoring of infection progression for a period of 1 month.

- the cost of the chemical sensor array is estimated to be about 15 cents per test and the smartphone attachment is about US$20 (excluding the phone).

Thank you